ACS OMEGA

Open Access

http://pubs.acs.org/journal/acsodf

Article

Qualitative and Quantitative Analysis of Azithromycin as Solid Dosage by Raman Spectroscopy

Muhammad Shahbaz,[‖] Ayesha Tariq,[‖] Muhammad Irfan Majeed,* Haq Nawaz,* Nosheen Rashid, Hina Shehnaz, Kiran Kainat, Hawa Hajab, Maryam Tahira, Noor ul Huda, Hira Tahseen, and Muhammad Imran

Cite This: *ACS Omega* 2023, 8, 36393−36400

Read Online

ACCESS | Metrics & More | Article Recommendations

ABSTRACT: Active pharmaceutical ingredients (APIs) and excipients are main drug constituents that ought to be identified qualitatively and quantitatively. Raman spectroscopy is aimed to be an efficient technique for pharmaceutical analysis in solid dosage forms. This technique can successfully be used in terms of qualitative and quantitative analysis of pharmaceutical drugs, their APIs, and excipients. In the proposed research, Raman spectroscopy has been employed to quantify Azithromycin based on its distinctive Raman spectral features by using commercially prepared formulations with altered API concentrations and excipients as well. Along with Raman spectroscopy, principal component analysis and partial least squares regression (PLSR), two multivariate data analysis techniques have been used for the identification and quantification of the API. For PLSR, goodness of fit of the model (R^2) was found to be 0.99, whereas root mean square error of calibration was 0.46 and root mean square error of prediction was 2.42, which represent the performance of the model. This study highlights the efficiency of Raman spectroscopy in the field of pharmaceutics by preparing pharmaceutical formulations of any drug to quantify their API and excipients to compensate for the commercially prepared concentrations.

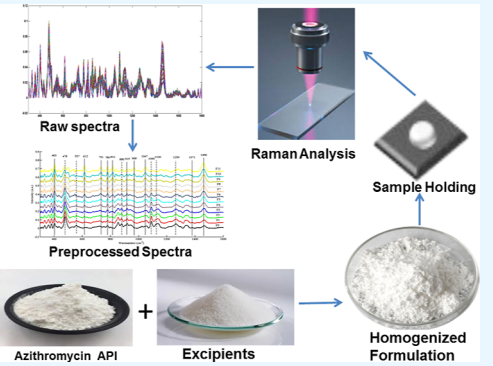

1. INTRODUCTION

Azithromycin (AZM), possessing the molecular formula $C_{38}H_{72}N_2O_{12}$, is found in the form of white crystalline powder and is a semisynthetic macrolide,[1] acid-stable, broad-spectrum,[2] and second-generation antibiotic with improved pharmacokinetic properties.[3−5] The pharmacokinetic properties involve a large area of drug absorption, metabolism, and excretion. The role of antimicrobial pharmacokinetics is to improve therapeutic efficiency and decrease drug toxicity.[6] It is a moderately water-soluble drug, having a molecular weight of 748.984 g/mol.[7] AZM is availed to treat many bacterial infections, namely, respiratory tract infections, sexually transmitted disease, skin infections, and soft tissue infections.[8]

AZM is commercially available in 250 and 500 mg tablets. On the other hand, its oral suspensions with concentrations of 100 and 200 mg/5 mL are also available commercially.[9] It is effective against many Gram-positive and Gram-negative bacteria including *Legionella pneumophila*, *Haemophilus influenzae*, and *Branhamella catarrhalis*.[10,11] AZM forbids the translation of mRNA in bacteria by interrupting the synthesis of protein and hence hinders bacterial growth.[12]

There is a need to analyze pharmaceutical formulations of AZM qualitatively and quantitatively. The absorption of AZM in raw materials, biological samples, and pharmaceutical formulations is determined by many techniques, such as high-performance liquid chromatography (HPLC),[13,14] mass spectrometry (MS),[15] Fourier transform infrared spectroscopy,[16] UV−vis spectroscopy,[17] LC−MS,[18] and electrochemical methods.[19,20] All above mentioned methods have some limitations such as being inflated, time-consuming, requiring rigorous sample preparation, and being laborious. In comparison to UV−vis spectrometry, Raman scattering is preferable as it is perceived in a single-beam mode which uses no reference channel to minimize instrumental sensitivity.

Raman spectroscopy is superior to the above-mentioned techniques because it is rapid, noninvasive, and requires little sample preparation. Raman spectroscopy is an efficient tool to characterize active pharmaceutical ingredients (APIs) in pharmaceutics due to polymorphism. It can also discriminate between API and excipients of any pharmaceutical drug.[21] On the other hand, this technique was also used to characterize

Received: July 20, 2023
Accepted: September 4, 2023
Published: September 20, 2023

counterfeit drugs which were used for the treatment of erectile dysfunction.[22−24] Nowadays, Raman spectroscopy is emerging as the technique of choice for the analysis of pharmaceuticals due to its great perspective in solid dosage analysis.[25,26] In the analysis of drugs and their intermediates, Raman spectroscopy is applied to analyze the polymorphic structure of API, identification of excipients, and quality assurance of drugs.[27−30] This technique has also been successfully and efficiently availed to analyze Sitagliptin[31] and Cefixime.[32] This technique can also analyze chemical and physical morphs more efficiently as compared to other spectroscopic techniques.[33,34]

In the current study, solid dosage formulations of AZM are prepared by mixing API and excipients in a definite proportion and are analyzed by using Raman spectroscopy, as this technique is known to be cost-effective, sensitive, and noninvasive. Along with Raman spectroscopy, principal component analysis (PCA) and partial least-squares regression (PLSR) analysis have been employed which provide the efficiency of Raman spectroscopy. PCA is used for qualitative analysis, whereas PLSR is used for quantitative analysis of pharmaceutical drugs. This study will be beneficial for the establishment of Raman spectroscopy for qualitative and quantitative analysis of pharmaceutical formulations.

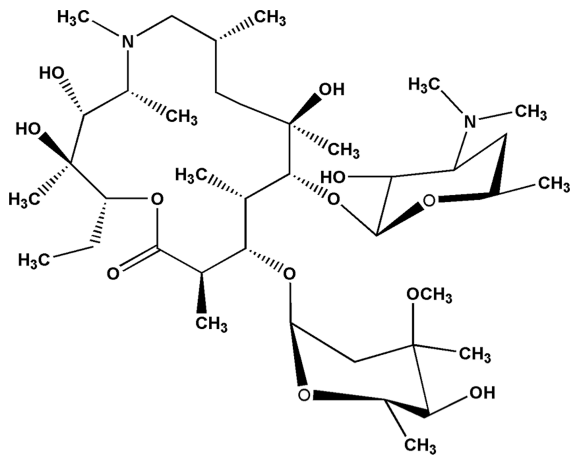

Figure 1. Chemical structure of AZM.

2. RESULTS AND DISCUSSION

2.1. Mean Raman Spectra. Figure 2 shows the mean Raman spectra of all samples of AZM with altered concentrations of API and excipients. The net concentration of each formulation is kept at 700 mg. The Raman spectral peak assignments, which are represented by solid and dotted lines, exhibit the difference in the peaks of the mean Raman spectra. The spectral peaks which are represented by dotted lines are related to excipients, which shows that the quantity of excipients in each successive formulation is decreasing gradually when observing from bottom to top, whereas the ones represented by solid lines are associated with API. This means that the quantity of API is increasing gradually in each successive formulation when observing from bottom to top. The differences in the mean Raman spectral peaks are related to increasing and decreasing concentrations of API and excipients, respectively, which are specified in Table 3, and their peak differences are exhibited in Table 1. The mean Raman spectrum which is labeled as A0 is associated with the pure excipient while the changing concentrations of excipients and API are labeled as A1−A10, and the Raman spectrum of pure API is labeled as A11, as shown in Figure 1.

As the API concentration increases, Raman spectral features with increasing intensities were observed at 1454, 1042, 963, 908, 811, 774, 731, 612, and 403 cm^{-1}. The intensities of these Raman spectral features increase with an increase in API concentration. The increase observed in the peaks of Raman spectral features of API is due to the polymorphic structure of API which can be polarized easily. A sharp Raman peak intensity at about 1454 cm^{-1} is due to stretching modes of the vibration of ether. The medium peak intensity at 1042 cm^{-1} is due to the stretching vibrations of C−C. A very weak Raman peak at 1371 cm^{-1} is due to the wagging vibration of the CH_2 group. A medium peak intensities at 1042 and 963 cm^{-1} are allotted to the stretching of C−C and C═O, respectively. Slightly lower peak intensity at 908 cm^{-1} represents the C−N−C torsion vibration. The medium Raman peak intensities at 811 and 774 cm^{-1} are due to C−C and C−N stretching vibrations of AZM, respectively. The vibrations detected at 731 cm^{-1} are C−O−C out of plane vibrations. The medium Raman peak intensities at about 612 and 403 cm^{-1} are associated with C−OH and C−C−C bending vibrations, respectively.

Furthermore, Raman spectral features at 1259, 1126, 1083, 876, 557, and 478 cm^{-1} are found to be of excipients, with a gradual decrease observed in their peaks. The gradual decrease detected in the Raman spectral peaks of excipients is due to their aliphatic structure. A very weak Raman spectral peak observed at 1259 cm^{-1} is due to the C−H deformation vibration of sucrose which is used as a filler in pharmaceutical formulations. Other weak Raman peaks at 1126 and 557 cm^{-1} represent stretching vibrations of starch and calcium phosphate, respectively, which are used as diluents in solid dosage forms. The medium Raman intensity peaks at 1083 and 876 cm^{-1} characterize lactose vibrations and C−C═O deformation in pectin, respectively. The C−C scissoring vibrations can be observed prominently at 478 cm^{-1}.

2.2. Principle Component Analysis. PCA is used to distinguish between various absorptions of solid dosage forms of AZM based on Raman spectral data sets. Raman spectral data of each concentration was used to perform PCA which can identify API as well as excipients of each AZM formulation.[42] Figure 3 shows the PCA plot of pure API (A11) and pure excipients (A0) along with various concentrations of solid dosage forms of AZM. In this figure, it can be seen clearly that formulations of various concentrations are differentiated from each other as the API concentration increases. The formulations of various concentrations are differentiated as positive and negative principal components. Specifically, the PCA plot discriminates all groups of various concentrations of AZM in order from A0−A11, describing 84.95% variability by PC-1 and remaining 6.13% variability by PC-2.

Figure 4 represents the PCA analysis of Raman spectral data sets of formulations A1 and A10 showing the differentiation in the form of clusters on positive as well as negative axis, while PCA loadings are explained in Figure 5 which is the reason for this separate spectral clustering.

https://doi.org/10.1021/acsomega.3c05245
ACS Omega 2023, 8, 36393−36400

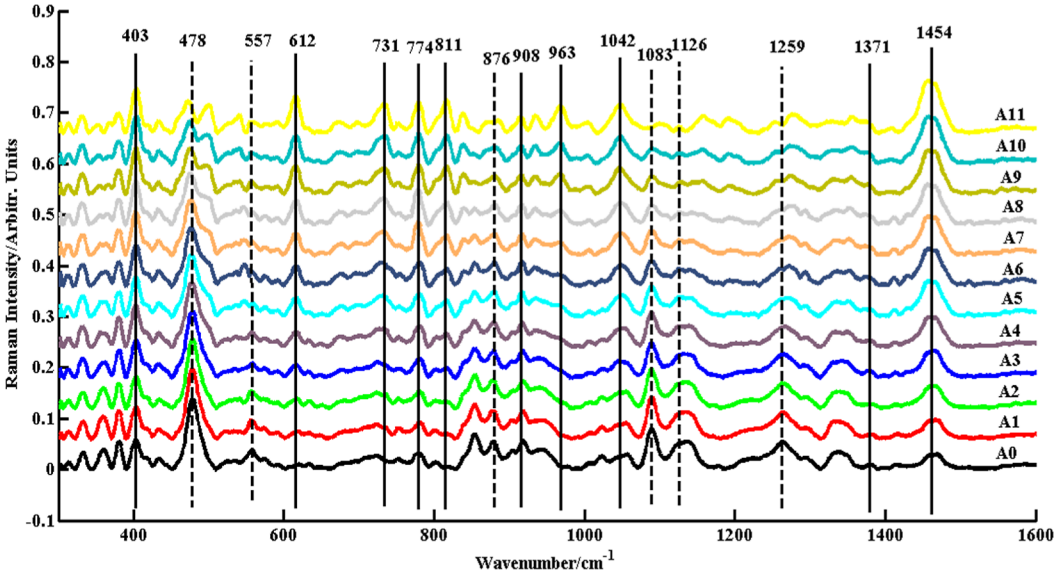

Figure 2. Mean Raman spectra of 12 formulations of AZM.

Table 1. Peaks Assignment of Raman Spectral Features Detected in the Mean Spectra of AZM

Raman peak position (cm^{-1})	peak assignment	references
403	C−N−C deformation	31
478	CC scissoring	32
557	calcium phosphate	35
612	C−OH bending	36
731	C−O−C out of plane	36
774	=C−N stretching	36
811	C−C stretching	36
876	C−C=O deformation	37
908	C−N−C torsion	36
963	C=O stretching	36
1042	C−C stretching	36
1083	lactose vibrations	38
1126	wheat starch stretching	39
1259	C−H deformation of sucrose	40
1371	CH_2 wagging	36
1454	C−O−C stretching	41

Table 2. Estimation of Blind Concentrations of Certain Unknown Samples by PLSR

sample name	calculated conc	predicted conc	RMSEC %	RMSEP %
A2	100	102.56	2.31	2.68
A4	200	203.43	2.46	2.85
A6	300	303.38	1.92	2.34
A8	400	402.87	2.02	3.14
A10	500	503.68	2.57	2.79

In Figure 5, PC loadings are discussed. There are positive and negative loadings. The Raman spectral peaks appearing in positive loadings refer to the peaks of API, whereas the Raman spectral peaks appearing in negative loadings are referred to as peaks of excipients. PC loadings confirm the peaks assignments in the mean plot in Figure 2. PC-loadings of API as well as excipients are sorted by solid lines and are associated with positive and negative loadings, respectively.

The Raman spectral features which are detected in PC-1 regarding positive loadings comprise 1456 cm^{-1} (C−O−C stretching mode), 1375 cm^{-1} (CH_2 wagging), 1042 cm^{-1} (C=C stretching), 966 cm^{-1} (C=O stretching), 811 cm^{-1} (C−C str.), 778 cm^{-1} (C−O−C torsion), 735 cm^{-1} (C−O−C out of plane), 616 cm^{-1} (C−O−C bending), and 403 cm^{-1} (C−N−C bending), which appeared prominently and are assigned to API of AZM. The spectral features which are detected in PC-1 regarding negative loadings are at 1262 cm^{-1} (C−H deformation), 1083 cm^{-1} (lactose vibrations), 880 cm^{-1} (C−C=O torsion), and 558 cm^{-1} (calcium phosphate vibrations) and are related to excipients. Hence, PCA scatter plots with respect to loadings are successfully used to discriminate the spectral features of API and excipients as well.

Table 3. 12 Formulations with Alternating Concentrations of API and Excipients in Solid Dosage Forms

s. no	sample name	excipient (mg)	API (mg)	net weight (mg)
1	A0	700	0	700
2	A1	650	50	700
3	A2	600	100	700
4	A3	550	150	700
5	A4	500	200	700
6	A5	450	250	700
7	A6 (unknown)	400	300	700
8	A7	350	350	700
9	A8	300	400	700
10	A9	250	450	700
11	A10	200	500	700
12	A11	0	700	700

2.3. Partial Least Squares Regression Analysis. PLSR is a multivariate data analysis technique that is used to predict different API concentrations in different solid dosage formulations on the basis of their specific Raman spectral features. To perform PLSR, the prediction models are constructed by using standard samples that contain known concentrations of AZM. For this purpose, the PLSR model consists of two steps, including calibration and validation models, which are performed by the randomization of Raman spectral data attained from standard samples (A0−A11) to divide the samples into two sets.

https://doi.org/10.1021/acsomega.3c05245
ACS Omega 2023, 8, 36393−36400

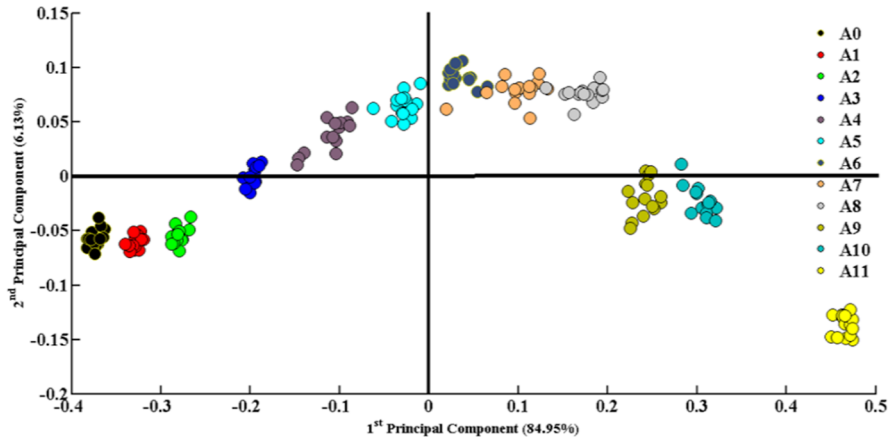

Figure 3. PCA plot of Raman spectra of various formulations of AZM.

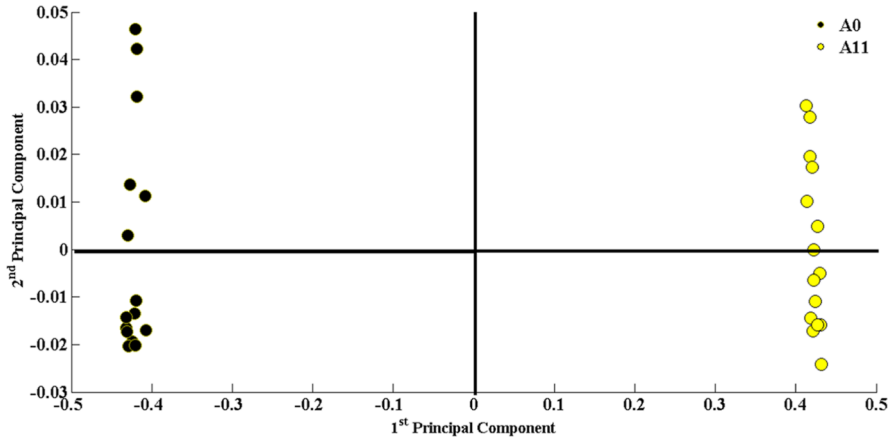

Figure 4. Comparison of PCA plots of pure API (A11) vs pure excipients (A0).

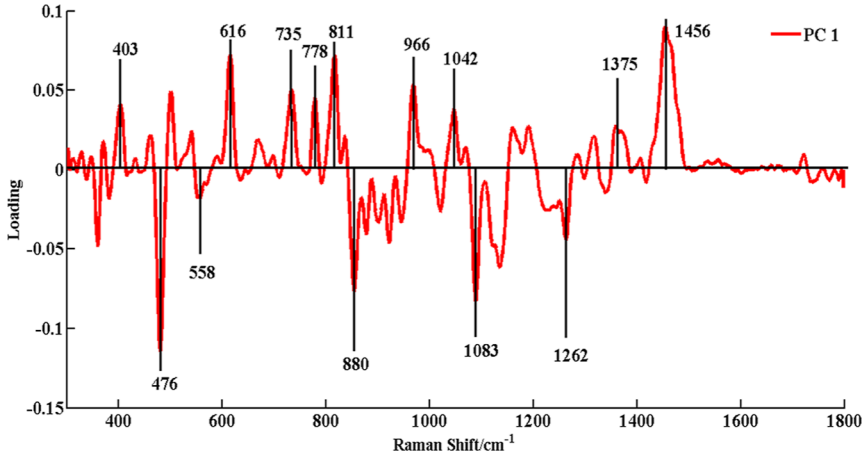

Figure 5. PC loadings of Raman spectral data for the first principal component (PC-1) of AZM.

Figure 6 represents the root-mean-square error cross validation (RMSECV) and root-mean-square error of calibration (RMSEC) of the first 7 latent variables (LVs). In the PLSR model, the optimum number of LVs has great importance. A few or too many LVs can affect the prediction ability of PLSR calibration and validation models. Generally, the optimum numbers of LVs are those numbers where the minimum RMSECV and RMSEC values are extended. So, for this purpose, 5 LVs are selected which provide an RMSEC of 0.46. From Figure 5, no significant improvement in the model has been seen after 5 LVs. The purpose of constructing this PLSR model is to predict the standards of API concentrations in solid dosage forms of AZM.

2.3.1. Root Mean Square Error of Calibration. The optimal number of LVs is 5, showing the distinct prediction of various drug concentrations with an unknown concentration. The RMSEC is 0.46. Figure 7 presents the regression model for 5 LVs which indicate the predicted concentration as the true concentration. The value of R^2 appeared to be 0.99, which describes the goodness of the model.

https://doi.org/10.1021/acsomega.3c05245
ACS Omega 2023, 8, 36393−36400

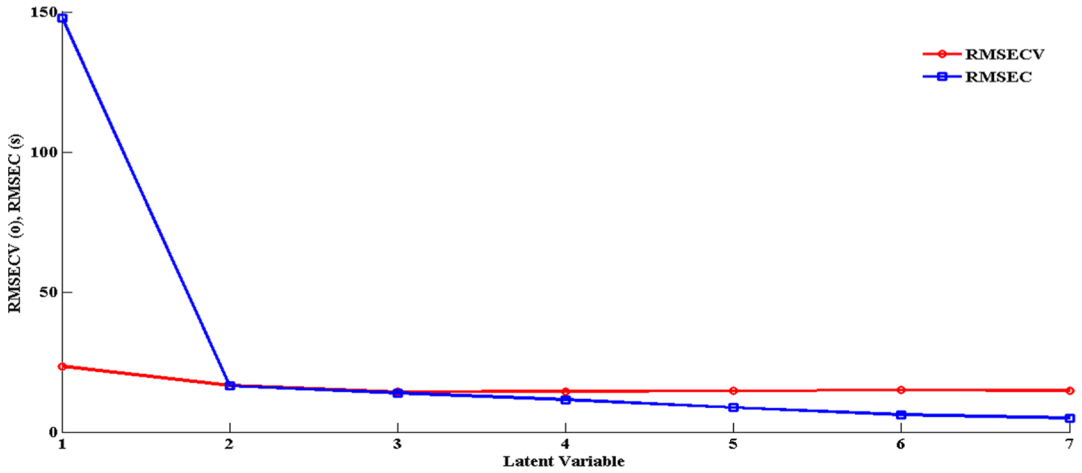

Figure 6. Presentation of the PLSR model of AZM to predict the number of latent variables.

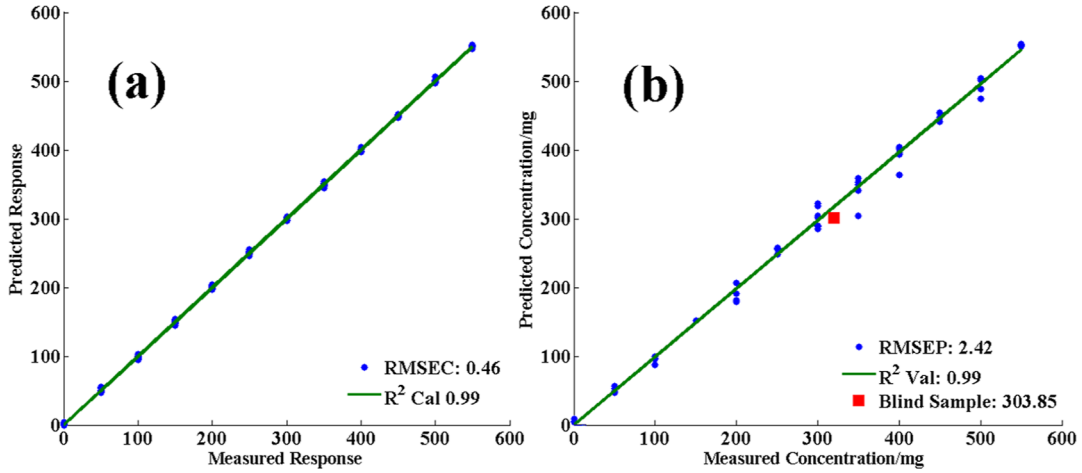

Figure 7. Presentation of PLSR analysis with (a) calibration and (b) prediction values of Raman spectral data for the quantification of AZM.

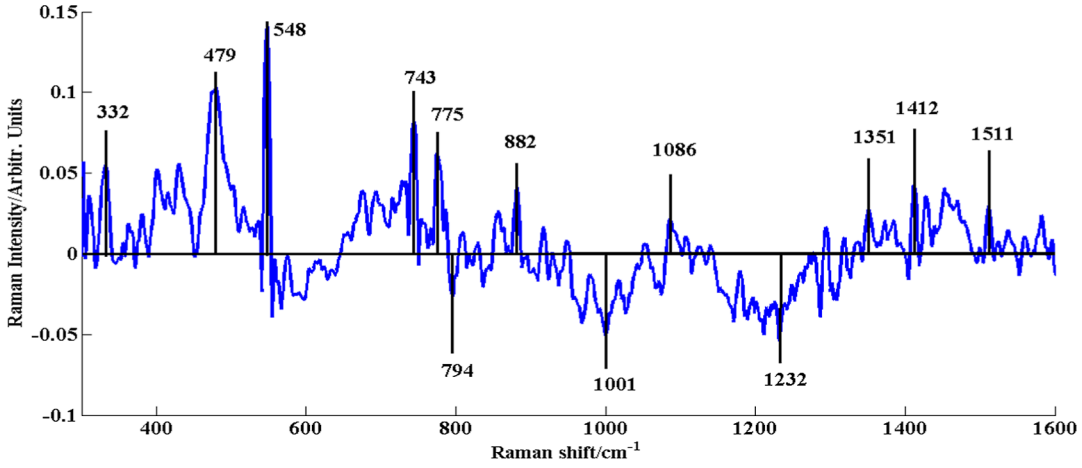

Figure 8. Regression coefficients of PLSR analysis of solid dosage formulations of AZM.

2.3.2. Prediction of Unknown Concentrations. Figure 7b shows the unknown concentration of the drug quantitatively, designated by a small red block, and it is predicted to be about 303.85 mg. The estimation of some randomly selected samples using the PLSR model is listed in Table 2. The PLSR model is specifically used for the quantification of unknown concentrations of solid dosage formulations of the pharmaceutical.

2.3.3. Regression Coefficients. Figure 8 represents the regression coefficients which are attained via the PLSR model. The peaks which are associated with the positive side are 332, 479, 548, 743, 775, 882, 1086, 1351, 1412, and 1511 cm^{-1}, and these are related to API as detected in Figure 5 and already discussed above. The peaks that are associated with the

https://doi.org/10.1021/acsomega.3c05245
ACS Omega 2023, 8, 36393−36400

negative side are 794, 1001, and 1232 cm^{-1} and are related to the excipients.

3. MATERIALS AND METHOD

3.1. Sample Preparation. The API of AZM was taken from Getz Pharma (Pvt) Ltd., Lahore, Pakistan. The solid dosage formulations of AZM were prepared by mixing the excipients, which contain talcum powder, starch, lactulose, and titanium powder with the AZM API in different concentrations. All formulations formed by mixing API and excipients were homogenized in powder form. Almost 30 mg of each formulation/sample was kept on an aluminum substrate. Fifteen Raman spectra were obtained for each sample. While recording the Raman spectra of each sample, the objective 4× was fixed at various locations of the sample in order to address the homogeneity of each sample.

3.2. Raman Spectral Acquisition. The spectral acquisition of various samples of AZM was done by a Raman spectrometer (Peak Seeker Pro-785; Agiltron, USA). About 30 mg of sample was put on an aluminum slide from each formulation at standard temperature; a 785 nm laser was applied as an excitation source via a 4× objective. To record the signal, a charged coupled detector was used in an apparatus that reduces electrical noise in the spectra. From each formulation mentioned in Table 3 (A0−A11), 15 Raman spectra were obtained. In this way, a total of 180 Raman spectra were acquired for 12 formulations of solid dosage forms with spectral sequences of 200−1600 cm^{-1}.

While preprocessing the Raman spectral data by using the software named MatLab, 1 formulation (A6) among 12 formulations was kept unknown to confirm the strength of the PLSR model for quantitative analysis. After all spectra were recorded, Raman spectral data sets were introduced to MatLab 7.8 (.dat files) for data preprocessing and multivariate analysis.

3.3. Data Preprocessing. To preprocess the Raman spectral data of the various samples of AZM, MatLab 7.8 (The MathWorks Inc., Natwick, MA, USA)[43] with in-house-developed codes was applied. The preprocessing involved substrate removal, baseline correction and smoothing, and vector normalization methods. For the smoothing process, the Savitzky−Golay filter was used.[44] Furthermore, spectra of the substrate (aluminum peak) were subtracted from each spectrum of various concentrations/formulations of AZM, and for baseline correction, a rubber band algorithm was used.

3.4. Data Analysis. Raman spectral features were analyzed by plotting the mean spectra of all samples containing various concentrations of API as well as excipients.[44] To elucidate the Raman spectral features of AZM, peak assignments were taken from the literature and are assigned in Table 1. PCA is basically used for quantitative analysis where the variables analyzed are numerical. On the other hand, PCA can also be used for qualitative analysis where the text data is transformed into numerical vectors. In the current study, PCA is utilized for the qualitative analysis of AZM.[45] The main objective of PCA is to reduce the complexity of high dimensional data. The PCA scatter plot transforms correlated variables into uncorrelated variables to minimize the proportionality of data as well as its variability.[46] The extreme variability is elucidated by the first principal component (PC-1), whereas the residual variability is elucidated by the second principal component (PC-2).[47] PLSR is used for quantitative analysis as well as to attain information about the covariance and known concentrations of spectral data of various forms of AZM.[48] The PLS regression analysis was used in two steps, including calibration and validation of the spectral data sets. From the calibration step, the relevant information on prediction is attained, whereas for validation step, newly explored components are utilized to check the presentation of regression model. For this purpose, leave one sample out cross validation is applied in the validation model.

4. CONCLUSIONS

Raman spectroscopy along with PCA and PLSR analysis has been found to be a very efficient technique for pharmaceutical analysis. In the solid dosage formulations of various concentrations of AZM, PCA is used to discriminate API and excipients, whereas PLSR is used for the quantification of API and excipients. In comparison to other techniques, Raman spectroscopy is more useful as it provides detailed information about composition of the pharmaceutical formulations, requires minimal or no sample preparation, and provides information about all components of formulations without their separation. Moreover, in solid dosage forms of a pharmaceutical drug, Raman spectroscopy is useful for both qualitative and quantitative analysis using characteristic Raman spectral features of the API. As compared to other techniques, Raman spectra can be collected from samples with less acquisition time. Raman spectroscopy successfully identified the spectral features of API of the AZM at 1454, 1042, 963, 908, 811, 774, 731, 612, and 403 cm^{-1}. Basically, this technique can be utilized for qualitative and quantitative evaluations of API of AZM in various concentrations of pharmaceutical formulations. In order to get quantitative analysis, the PLSR model was built where RMSEC and RMSEP values were 0.46 and 2.42, respectively.

AUTHOR INFORMATION

Corresponding Authors

Muhammad Irfan Majeed − *Department of Chemistry, University of Agriculture Faisalabad, Faisalabad 38000, Pakistan;* orcid.org/0000-0003-0506-6060; Phone: 0092-304-7066369; Email: irfan.majeed@uaf.edu.pk

Haq Nawaz − *Department of Chemistry, University of Agriculture Faisalabad, Faisalabad 38000, Pakistan;* orcid.org/0000-0003-2739-4735; Phone: 0092-306-4735084; Email: haqchemist@yahoo.com

Authors

Muhammad Shahbaz − *Department of Chemistry, University of Agriculture Faisalabad, Faisalabad 38000, Pakistan*

Ayesha Tariq − *Department of Chemistry, University of Agriculture Faisalabad, Faisalabad 38000, Pakistan*

Nosheen Rashid − *Department of Chemistry, University of Education, Faisalabad 38000, Pakistan*

Hina Shehnaz − *Department of Chemistry, University of Agriculture Faisalabad, Faisalabad 38000, Pakistan*

Kiran Kainat − *Department of Chemistry, University of Agriculture Faisalabad, Faisalabad 38000, Pakistan*

Hawa Hajab − *Department of Chemistry, University of Agriculture Faisalabad, Faisalabad 38000, Pakistan*

Maryam Tahira − *Department of Chemistry, University of Agriculture Faisalabad, Faisalabad 38000, Pakistan*

Noor ul Huda − *Department of Chemistry, University of Agriculture Faisalabad, Faisalabad 38000, Pakistan*

Hira Tahseen − *Department of Chemistry, University of Agriculture Faisalabad, Faisalabad 38000, Pakistan*

https://doi.org/10.1021/acsomega.3c05245
ACS Omega 2023, 8, 36393−36400

Muhammad Imran − *Department of Chemistry, Faculty of Science, King Khalid University, Abha 61413, Saudi Arabia*

Complete contact information is available at: https://pubs.acs.org/10.1021/acsomega.3c05245

Author Contributions

[‖]M.S. and A.T. have equal contribution.

Funding

M. Imran expresses his appreciation to the Deanship of Scientific Research at King Khalid University, Saudi Arabia, for funding this work through research group program under grant number R.G.P. 2/522/44.

Notes

The authors declare no competing financial interest.

REFERENCES

(1) Ciftci, D.; Ubeyitogullari, A.; Huerta, R. R.; Ciftci, O. N.; Flores, R. A.; Saldaña, M. D. Lupin hull cellulose nanofiber aerogel preparation by supercritical CO2 and freeze drying. *J. Supercrit. Fluids* **2017**, *127*, 137−145.

(2) Firth, A.; Prathapan, P. Azithromycin: the first broad-spectrum therapeutic. *Eur. J. Med. Chem.* **2020**, *207*, 112739−739.

(3) Kong, F. Y.; Rupasinghe, T. W.; Simpson, J. A.; Vodstrcil, L. A.; Fairley, C. K.; McConville, M. J.; Hocking, J. S. Pharmacokinetics of a single 1g dose of azithromycin in rectal tissue in men. *PLoS One* **2017**, *12* (3), No. e0174372.

(4) Davidson, R. J. In vitro activity and pharmacodynamic/pharmacokinetic parameters of clarithromycin and azithromycin: why they matter in the treatment of respiratory tract infections . *Infect. Drug Resist.* **2019**, *12*, 585−596.

(5) Ghari, T.; Kobarfard, F.; Mortazavi, S. A. Development of a Simple RP-HPLC-UV Method for Determination of Azithromycin in Bulk and Pharmaceutical Dosage forms as an Alternative to the USP Method. *Iran. J. Pharm. Res.* **2013**, *12*, 57.

(6) Kong, F. Y. S.; Horner, P.; Unemo, M.; Hocking, J. S. Pharmacokinetic considerations regarding the treatment of bacterial sexually transmitted infections with azithromycin: a review. *J. Antimicrob. Chemother.* **2019**, *74* (5), 1157−1166.

(7) Jaiswar, D. R.; Jha, D.; Amin, P. D. Preparation and characterizations of stable amorphous solid solution of azithromycin by hot melt extrusion. *J. Pharm. Invest.* **2016**, *46*, 655−668.

(8) Li, Y.; Du, G.; Cai, W.; Shao, X. Classification and quantitative analysis of Azithromycin tablets by Raman spectroscopy and chemometrics. *Am. J. Anal. Chem.* **2011**, *02* (02), 135−141.

(9) Curatolo, W.; Foulds, G.; LaBadie, R. Mechanistic study of the azithromycin dosage-form-dependent food effect. *Pharm. Res.* **2010**, *27*, 1361−1366.

(10) Peters, D. H.; Friedel, H. A.; McTavish, D. Azithromycin: a review of its antimicrobial activity, pharmacokinetic properties and clinical efficacy. *Drugs* **1992**, *44* (5), 750−799.

(11) Barry, A. L.; Jones, R.; Thornsberry, C. In vitro activities of azithromycin (CP 62,993), clarithromycin (A-56268; TE-031), erythromycin, roxithromycin, and clindamycin. *J. Antimicrob. Chemother.* **1988**, *32* (5), 752−754.

(12) Bakheit, A.; Al-Hadiya, B.; Abd-Elgalil, A. Azithromycin. *Profiles Drug Subst. Excipients Relat. Methodol.* **2014**, *39*, 1−40.

(13) Sharmin, N.; Shanta, N. S.; Bachar, S. C. Spectrophotometric analysis of Azithromycin and its pharmaceutical dosage forms: Comparison between Spectrophotometry and HPLC. *Dhaka Univ. J. Pharm. Sci.* **2015**, *12* (2), 171−179.

(14) Al-Hakkani, M. F. A rapid, developed and validated RP-HPLC method for determination of azithromycin. *SN Appl. Sci.* **2019**, *1* (3), 222.

(15) Mousavi, S. H. H.; Kobarfard, F.; Husain, S. W.; Tehrani, M. S.; Azar, P. A.; Ahmadkhaniha, R.; Mehdizadeh, A. A rapid, simple, liquid chromatographic-electrospray ionization, ion trap mass spectrometry method for the determination of finasteride in human plasma and its application to pharmacokinetic study. *Iran. J. Pharm. Res.* **2012**, *11* (1), 59.

(16) Mallah, M. A.; Sherazi, S.; Mahesar, S. A.; Rauf, A. Assessment of azithromycin in pharmaceutical formulation by fourier-transform infrared (FT-IR) transmission spectroscopy. *Pak. J. Anal. Environ. Chem.* **2011**, *12* (1 & 2), 7.

(17) Suhagia, B.; Shah, S.; Rathod, I.; Patel, H.; Doshi, K. Determination of Azithromycin in pharmaceutical dosage forms by Spectrophotometric method. *Indian J. Pharm. Sci.* **2006**, *68* (2), 242.

(18) Vodstrcil, L. A.; Rupasinghe, T. W.; Kong, F. Y.; Tull, D.; Worthington, K.; Chen, M. Y.; Huston, W. M.; Timms, P.; McConville, M. J.; Fairley, C. K.; et al. Measurement of tissue azithromycin levels in self-collected vaginal swabs post treatment using liquid chromatography and tandem mass spectrometry (LC-MS/MS). *PLoS One* **2017**, *12* (5), No. e0177615.

(19) Sharma, T. S. K.; Hwa, K.-Y. Architecting hierarchal Zn3V2O8/P-rGO nanostructure: Electrochemical determination of anti-viral drug azithromycin in biological samples using SPCE. *Chem. Eng. J.* **2022**, *439*, 135591.

(20) Guerra, E.; Cestarolli, D. Azithromycin electrochemical detection using a VO2 thin film. *J. Alloys Compd.* **2021**, *885*, 160997.

(21) Tuschel, D. Raman spectroscopy and polymorphism. *Spectroscopy* **2019**, *34* (3), 10−21.

(22) Sanada, T.; Yoshida, N.; Kimura, K.; Tsuboi, H. Discrimination of falsified erectile dysfunction medicines by use of an ultra-compact Raman scattering spectrometer. *Pharm.* **2020**, *9* (1), 3.

(23) Bottoni, P.; Caroli, S. Fake pharmaceuticals: A review of current analytical approaches. *Microchem. J.* **2019**, *149*, 104053.

(24) Sanada, T.; Yoshida, N.; Kimura, K.; Tsuboi, H. Detection method of falsified medicines by using a low-cost Raman scattering spectrometer combined with soft independent modeling of class analogy and partial least squares discriminant analysis. *Biol. Pharm. Bull.* **2021**, *44* (5), 691−700.

(25) Glover, W. B. N-beta-methylamino-L-alanine: a non-protein amino acid incorporated into protein. M.Sc. Thesis, University of British Columbia, 2014.

(26) Strachan, C. J.; Rades, T.; Gordon, K. C.; Rantanen, J. Raman spectroscopy for quantitative analysis of pharmaceutical solids. *J. Pharm. Pharmacol.* **2010**, *59* (2), 179−192.

(27) Cailletaud, J.; De Bleye, C.; Dumont, E.; Sacré, P. Y.; Netchacovitch, L.; Gut, Y.; Boiret, M.; Ginot, Y.-M.; Hubert, P.; Ziemons, E. Critical review of surface-enhanced Raman spectroscopy applications in the pharmaceutical field. *J. Pharm. Biomed. Anal.* **2018**, *147*, 458−472.

(28) Hédoux, A.; Guinet, Y.; Descamps, M. The contribution of Raman spectroscopy to the analysis of phase transformations in pharmaceutical compounds. *Int. J. Pharm.* **2011**, *417* (1−2), 17−31.

(29) Vankeirsbilck, T.; Vercauteren, A.; Baeyens, W.; Van der Weken, G.; Verpoort, F.; Vergote, G.; Remon, J. P. Applications of Raman spectroscopy in pharmaceutical analysis. *TrAC, Trends Anal. Chem.* **2002**, *21* (12), 869−877.

(30) Ayala, A. P. Polymorphism in drugs investigated by low wavenumber Raman scattering. *Vib. Spectrosc.* **2007**, *45* (2), 112−116.

(31) Bakkar, M. A.; Nawaz, H.; Majeed, M. I.; Naseem, A.; Ditta, A.; Rashid, N.; Ali, S.; Bajwa, J.; Bashir, S.; Ahmad, S.; et al. Raman spectroscopy for the qualitative and quantitative analysis of solid dosage forms of Sitagliptin. *Spectrochim. Acta Mol. Biomol. Spectrosc.* **2021**, *245*, 118900.

(32) Bajwa, J.; Nawaz, H.; Majeed, M. I.; Hussain, A. I.; Farooq, S.; Rashid, N.; Bakkar, M. A.; Ahmad, S.; Hyat, H.; Bashir, S.; et al. Quantitative analysis of solid dosage forms of cefixime using Raman spectroscopy. *Spectrochim. Acta Mol. Biomol. Spectrosc.* **2020**, *238*, 118446.

(33) D Patel, B.; J Mehta, P. An overview: application of Raman spectroscopy in pharmaceutical field. *Curr. Pharm. Anal.* **2010**, *6* (2), 131−141.

(34) Lipiäinen, T.; Fraser-Miller, S. J.; Gordon, K. C.; Strachan, C. J. Direct comparison of low-and mid-frequency Raman spectroscopy for

quantitative solid-state pharmaceutical analysis. *J. Pharm. Biomed. Anal.* **2018**, *149*, 343−350.
(35) Kodati, V. R.; Tomasi, G. E.; Turumin, J. L.; Tu, A. T. Raman spectroscopic identification of phosphate-type kidney stones. *Appl. Spectrosc.* **1991**, *45* (4), 581−583.
(36) Santana, N. S.; Gomes, A. F.; Santana, H. S.; Saraiva, G. D.; Ribeiro, P. R.; Santos, A. O.; Nogueira, C. E.; de Sousa, F. F. Phase Transformations of Azithromycin Crystals Investigated by Thermal and Spectroscopic Analyses Combined with Ab Initio Calculations. *Cryst. Growth Des.* **2021**, *21*, 3602−3613.
(37) Tammer, M. G. *Sokrates: Infrared and Raman characteristic group frequencies: tables and charts*; Springer, 2004.
(38) Murphy, B. M.; Prescott, S. W.; Larson, I. Measurement of lactose crystallinity using Raman spectroscopy. *J. Pharm. Biomed. Anal.* **2005**, *38* (1), 186−190.
(39) De Gussem, K.; Vandenabeele, P.; Verbeken, A.; Moens, L. Raman spectroscopic study of Lactarius spores (Russulales, Fungi). *Spectrochim. Acta Mol. Biomol. Spectrosc.* **2005**, *61* (13−14), 2896−2908.
(40) Cerchiaro, G.; Sant'Ana, A. C.; Temperini, M. L. A.; da Ferreira, A. M. C. Investigations of different carbohydrate anomers in copper (II) complexes with D-glucose, D-fructose, and D-galactose by Raman and EPR spectroscopy. *Carbohydr. Res.* **2005**, *340* (15), 2352−2359.
(41) Shende, C.; Smith, W.; Brouillette, C.; Farquharson, S. Drug stability analysis by Raman spectroscopy. *Pharm.* **2014**, *6* (4), 651−662.
(42) Amigo, J. M. Practical issues of hyperspectral imaging analysis of solid dosage forms. *Anal. Bioanal. Chem.* **2010**, *398* (1), 93−109.
(43) Nawaz, H.; Bonnier, F.; Knief, P.; Howe, O.; Lyng, F. M.; Meade, A. D.; Byrne, H. J. Evaluation of the potential of Raman microspectroscopy for prediction of chemotherapeutic response to cisplatin in lung adenocarcinoma. *Analyst* **2010**, *135* (12), 3070−3076.
(44) Nawaz, H.; Rashid, N.; Saleem, M.; Asif Hanif, M.; Irfan Majeed, M.; Amin, I.; Iqbal, M.; Rahman, M.; Ibrahim, O.; Baig, S.; et al. Prediction of viral loads for diagnosis of Hepatitis C infection in human plasma samples using Raman spectroscopy coupled with partial least squares regression analysis. *J. Raman Spectrosc.* **2017**, *48* (5), 697−704.
(45) Roggo, Y.; Edmond, A.; Chalus, P.; Ulmschneider, M. Infrared hyperspectral imaging for qualitative analysis of pharmaceutical solid forms. *Anal. Chim. Acta* **2005**, *535* (1−2), 79−87.
(46) Saade, J.; Pacheco, M. T. T.; Rodrigues, M. R.; Jr, L. S. Identification of hepatitis C in human blood serum by near-infrared Raman spectroscopy. *Spectroscopy* **2008**, *22* (5), 387−395.
(47) Deconinck, E.; Van Nederkassel, A.-M.; Stanimirova, I.; Daszykowski, M.; Bensaid, F.; Lees, M.; Martin, G.; Desmurs, J.; Smeyers-Verbeke, J.; Vander Heyden, Y. Isotopic ratios to detect infringements of patents or proprietary processes of pharmaceuticals: two case studies. *J. Pharm. Biomed. Anal.* **2008**, *48* (1), 27−41.
(48) Gabrielsson, J.; Lindberg, N. O.; Lundstedt, T. Multivariate methods in pharmaceutical applications. *J. Chemom.: J. Chemom. Soc.* **2002**, *16* (3), 141−160.

https://doi.org/10.1021/acsomega.3c05245
ACS Omega 2023, 8, 36393−36400